

EFFICIENT REPRESENTATION OF LIGHTING PATTERNS FOR IMAGE-BASED RELIGHTING

Hyunjung Shim

Tsuhan Chen

{hjs,tsuhan}@andrew.cmu.edu

Department of Electrical and Computer Engineering
Carnegie Mellon University
Pittsburgh, PA, 15213, USA

Abstract

Image-based relighting (IBL) has become a popular research topic in both computer graphics and signal processing. IBL is the technique that renders images of a scene under different lighting conditions without prior knowledge of the object geometry and surface properties in the scene. Simply put, IBL collects images of the scene under all possible lighting conditions and process these images to render an image of the scene under a new lighting condition. To be practical, IBL strives to reduce the number of images that need to be captured, and most IBL algorithms do so by estimating the surface reflectance function (SRF) of the scene, which represents the response of each pixel in the scene to lighting from various directions. IBL hence becomes the problem of estimating the SRF using a number of lighting patterns to illuminate the scene. To minimize the number of lighting patterns needed, we propose to use a statistical approach, principal component analysis (PCA), and show that the most efficient lighting patterns should be the eigenvectors of the covariance matrix of the SRFs, corresponding to the largest eigenvalues. In addition, we show that discrete cosine transform (DCT)-based lighting patterns perform as well as the optimal PCA-based lighting patterns for typical SRFs, especially for scenes with Lambertian surfaces. Both the PCA-based and the DCT-based methods outperform existing IBL algorithms with fewer lighting patterns.

1. INTRODUCTION

Within a couple of years, image-based relighting (IBL) has become a popular research topic in both computer graphics and signal processing. IBL collects images of the scene under all possible lighting conditions and processes these images to render an image of the scene under a new lighting condition. IBL has an advantage that prior knowledge of the object geometry and surface properties in the scene is not needed for rendering. IBL is applied to many applications such as realistic visualization of scenes in a virtual

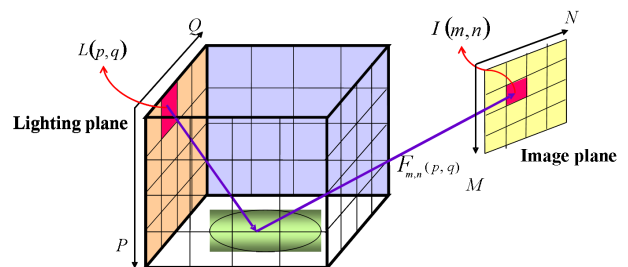


Figure 1: SRF model

environment and movie special effects.

1.1. Prior Work

Prior work for IBL essentially estimates, for each pixel of an image, a 2D light mapping function such as *plenoptic illumination function* [1], *reflected irradiance field* [2], *environment matte* [3, 4, 5], or *reflectance field* [6]. In this paper, we use the surface reflectance function (SRF) to unify all such 2D light mapping functions; the SRF is defined for each pixel in the scene image to represent the contribution of each point light source in the lighting plane (Figure 1), to the pixel in the image plane (Figure 1).

The first work that rendered an image as the linear combination of a set of basis images, was introduced by Nimeroff et al. [7]. Most traditional IBL methods focus on representation, sampling and compression issue after acquiring basis images [2, 1, 8, 9, 6]. Lin et al. [2] introduced the reflected irradiance field and solved the minimum sampling problem of the reflected irradiance field. Wong [1] extracted the lighting factor from the plenoptic function, calling it as the plenoptic illumination function. They also discussed how to compress the plenoptic illumination functions that were acquired from basis images. Ho

et al. [8] also proposed an algorithm to compress basis images, for IBL, based on principal component analysis (PCA) [10]. Masselus et al. [9] compared various interpolation techniques to improve the quality of rendered images. Debevec et al. [6] introduced the *Light Stage* to acquire the reflectance field of a human face. However, most of these techniques are often impractical due to the need of a large number of basis images, each corresponding to a lighting pattern. For example, for a 64×64 SRF, Lin et al. [2], Wong [1], Ho et al. [8] and Debevec et al. [6] needed 4096 basis images while [9] used 1024 basis images and interpolated given basis images for estimating the original SRF.

More recent work in IBL aims at the efficiency as well as the accuracy of estimating SRFs [3, 4, 5]. Zongker et al. [3] introduced an approach to estimating an environment matte (i.e., SRF) of specular and transparent scenes. They estimated an environment matte using basis images lit by Gray-coded lighting patterns. Chuang et al. [5] extended this technique for higher accuracy and real-time capturing. Instead of Gray-coded lighting patterns, they estimated matte parameters using basis images illuminated by Gaussian stripe patterns. They also provided a method to extract an environment matte from single basis image under certain scene constraints. Peers et al. [4] improved the efficiency of estimating an environment matte using wavelet lighting patterns. They measured the importance value of an applied pattern by computing the norm of the corresponding scene image. By learning from previously recorded images, they could select the most important lighting patterns among wavelets.

In [3, 4, 5], the choice of lighting patterns is based assumptions about the SRFs. Zongker et al. [3] selected Gray-coded lighting patterns since they assumed that an environment matte was a box function. They approximated an environment matte using tens of basis images. Chuang et al. [5] applied Gaussian stripe patterns because an environment matte was modelled as a Gaussian function. They used thousands of basis images to achieve higher accuracy of estimating an environment matte. Peers et al. [4] used wavelet basis functions for their lighting patterns because wavelet basis functions were known to be very effective for image coding and representation. They used from hundreds to thousands of basis images for estimating an environment matte.

The main contribution of our work is to show that selecting lighting patterns by learning from data statistics can significantly improve the efficiency of relighting with highly satisfying visual quality. Compared to [1, 2, 8], our work can be considered as a pre-compression technique for IBL since eventually we are able to reduce the number of basis images to be stored for IBL. Unlike Zongker et al. [3] and Chuang et al. [5], our proposed algorithm does not suffer from the complex computation caused by the optimization

process and the error caused by an incorrect initial model (e.g. a box function, a Gaussian function). Our work differs from [4] in that we design the lighting patterns based on data statistics of many SRFs, while lighting patterns in [4] are determined by each scene.

1.2. Overview

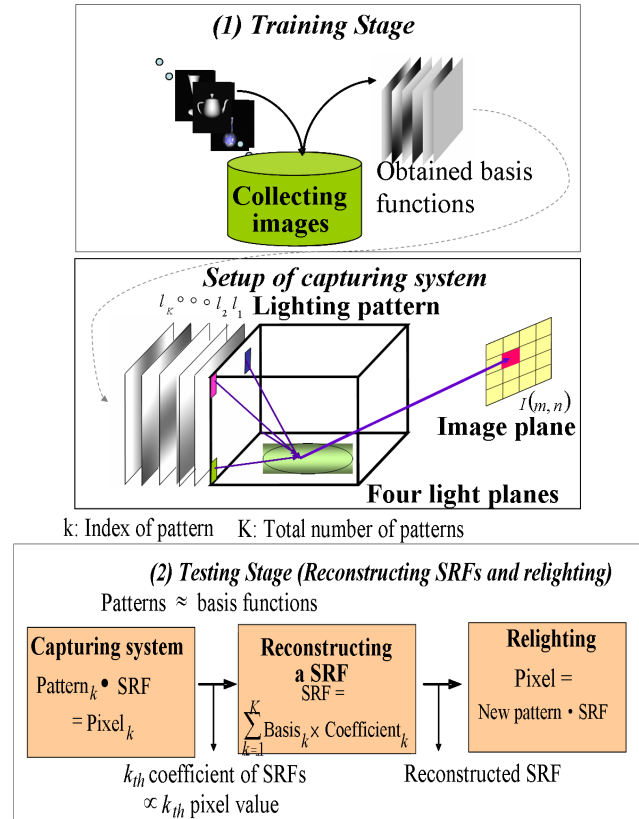


Figure 2: Flow of proposed algorithm

Our proposed algorithm has two stages: a training stage and a test stage (Figure 2).

First, for training, we collect SRF statistics from many synthetic images categorized by surface properties (Lambertian vs. specular). We apply PCA [10] to the SRFs (Figure 2.(1)) and show that SRFs are a highly correlated data set so that only a few eigenvectors can represent a wide range of possible SRFs. Based on this observation, we can simply choose the lighting patterns to be the eigenvectors of the covariance matrix of the SRFs.

Second, for testing, designed lighting patterns from the training stage (Figure 2.(1)) are applied to the scene to acquire basis images. Basis images are then used to synthesize the scene with novel lighting patterns (Figure 2.(2)).

It is interesting to note that the SRFs can be modelled as an Autoregressive(1) (AR(1)) process with a high correla-

tion parameter so that the PCA basis functions can be approximated by discrete cosine transform (DCT) basis functions [11]. In particular, SRFs from scenes with Lambertian surfaces fit better into an AR(1) model than SRFs from scenes with specular surfaces. We will see that DCT-based lighting patterns provide better performance for scenes with Lambertian surfaces than scenes with specular surfaces.

In the following section, we explain our algorithm for performing the reconstruction of SRFs from basis images and rendering an image using reconstructed SRFs (Section 2, Figure 2.(2)). Section 3 contains practical implementation issues. As a conclusion, we compare the performance of our reconstructed SRFs with other algorithms [3, 5, 4]. We also present the rendered images for our best result with the best result among [3, 5, 4] and images of same scene with true lighting (Section 4).

2. ALGORITHM DESCRIPTION

In this section, we derive the illumination of a pixel on the image plane with the rendering equation and develop a mathematical framework to estimate an SRF. An SRF is defined as a weighting function from light sources to the pixel value. In other words, the intensity value reflected by the surface is the inner product of an SRF and a lighting pattern [3, 5, 4, 7, 2, 6, 1].

$$I(m, n) = \sum_{p=1}^P \sum_{q=1}^Q F_{m,n}(p, q) L(p, q) \quad (1)$$

p, q : The index of the light plane, $p = 1 \dots P, q = 1 \dots Q$

m, n : The index of the image plane, $n = 1 \dots N, m = 1 \dots M$

$I(m, n)$: An intensity at (m, n) pixel where L is a corresponding lighting pattern

$F_{m,n}$: The SRF for pixel at $(m, n), 0 \leq F_{m,n} \leq 1$

$L(p, q)$: An incoming intensity at (p, q) from the light plane

We can cascade elements of an SRF function and a lighting pattern into vectors so that the rendering equation turns into Equation 2.

$$I(m, n) = \mathbf{F}^T \mathbf{L} \quad (2)$$

where \mathbf{F} is a $PQ \times 1$ vector and a \mathbf{L} is a $PQ \times 1$ vector. Our goal is to solve for \mathbf{F} , an SRF. Assuming that statistics of \mathbf{F} are given, we can obtain the most representative basis functions for \mathbf{F} using PCA [10]. That is, \mathbf{F} can be represented by linear combination of basis functions as follows (Equation 3).

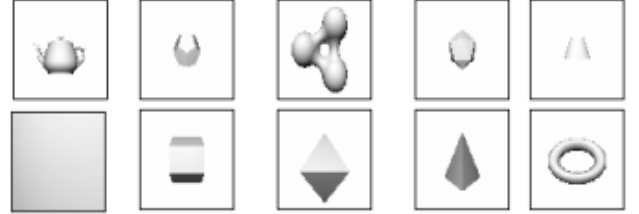
$$\mathbf{F} = c_1 \mathbf{e}_1 + c_2 \mathbf{e}_2 + \dots + c_{PQ} \mathbf{e}_{PQ} + \mathbf{m} \quad (3)$$

\mathbf{e}_k : k_{th} basis function

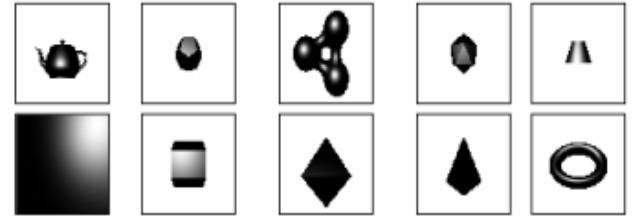
c_k : k_{th} coefficient corresponding to k_{th} basis function

\mathbf{m} : A mean vector from statistics

To obtain the most effective basis function, \mathbf{e}_k , we collect the statistics of \mathbf{F} and analyze it using PCA [10]. We obtain the statistics of \mathbf{F} from each set (Lambertian and Specular) of scenes rendered using ray tracing software (POV-RAY [12]) (Figure 2). We use ten different training scenes for each set classified by surface properties. Training scenes are shown as follows.



(1) Training scenes for Lambertian scenes



(2) Training scenes for Specular scenes

Figure 3: Training scenes

Performing PCA on the training data set, we observe that only a few basis functions dominate most of the energy distribution of the SRFs (Figure 4).

From the set of scenes with Lambertian surfaces, we find that 99.14% of energy is preserved within the first six eigenvectors. For the specular set, 70% of energy stays within the first six eigenvectors and 90% within the first 43 eigenvectors. Therefore, \mathbf{F} can be approximated by

$$\tilde{\mathbf{F}} \approx c_1 \mathbf{e}_1 + c_2 \mathbf{e}_2 + \dots + c_K \mathbf{e}_K + \mathbf{m}, K \ll PQ \quad (4)$$

Therefore, our goal becomes reconstructing \mathbf{F} using a minimum number of basis functions. To solve \mathbf{F} , we substitute \mathbf{L} in Equation 2 with \mathbf{e}_k .

$$\begin{aligned} I_k(m, n) &= (c_1 \mathbf{e}_1 + \dots + c_k \mathbf{e}_k + \dots + c_K \mathbf{e}_K + \mathbf{m})^T \mathbf{e}_k \\ &= c_k + \mathbf{m}^T \mathbf{e}_k \end{aligned} \quad (5)$$

Because basis functions are orthogonal to each other and they have unit norm, from Equation 6, a coefficient, c_k , is simply calculated from a radiance value at pixel (m, n) if a corresponding basis function \mathbf{e}_k is applied as the lighting pattern. In order to reconstruct \mathbf{F} without loss, we will need PQ basis functions. Thanks to PCA, we can select only a few basis functions, i.e., eigenvectors corresponding to the

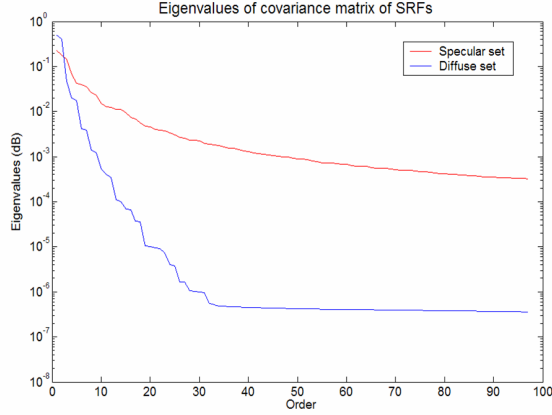


Figure 4: Eigenvalues of the covariance matrix of SRFs

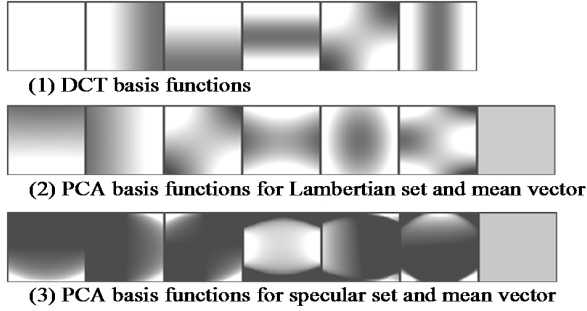


Figure 5: First six designed lighting patterns

largest eigenvalues. Six eigenvectors corresponding to the six largest eigenvalues and a mean vector from each set of statistics are shown in Figure 5 (1), (2), (3). If we collect enough data from many different scenes, we obtain a constant mean vector from PCA [10] as shown in Figure 5 (2), 5 (3). The first six DCT basis functions are shown in Figure 5 (1). From Figure 5, we observe that the basis functions from the Lambertian set have less contrast than the basis functions from the specular set of scenes. This is as expected because the SRFs from the Lambertian set have a wider and flatter characteristics than the SRFs from the specular set.

Equation 6 shows how to calculate coefficients corresponding to the basis functions. We apply calculated coefficients from Equation 6 to Equation 4 to obtain the reconstructed SRFs. Rendering a pixel is then done by simply computing the inner product with a novel lighting pattern as shown in the SRF as Equation 2. However, instead of computing and storing a reconstructed SRF, which often is a huge dimensional vector, we can simply keep coefficients, c_k , for each pixel and apply them for rendering a pixel directly ([4]). In other words, a rendered pixel value with a new lighting condition is calculated by

$$\begin{aligned} I_{new}(m, n) &= (c_1 \mathbf{e}_1 + \dots + c_k \mathbf{e}_k + \dots + c_K \mathbf{e}_K + \mathbf{m})^T \mathbf{L}_{new} \\ &= c_1 a_1 + \dots + c_K a_K + \mathbf{m}^T \mathbf{L}_{new} \end{aligned} \quad (6)$$

where $a_k = \mathbf{e}_k^T \mathbf{L}_{new}$.

3. IMPLEMENTATION DETAILS

In Section 2, we designed the optimal lighting patterns as basis functions of the covariance matrix of SRFs. To apply them as lighting patterns, we have to fit them into the range of an image. Since derived lighting patterns contain negative values and have a unit norm, it is necessary to scale and shift a basis function as follows.

$$\mathbf{L}_k = 255 \times \left(\frac{\mathbf{e}_k + |\min(\mathbf{E})| \mathbf{1}}{S_1} \right) \quad (7)$$

where \mathbf{k} is the index of the basis, \mathbf{e}_k is a \mathbf{k}_{th} basis function, \mathbf{E} is a basis matrix $[\mathbf{e}_1 \mathbf{e}_2 \dots \mathbf{e}_K]$, \mathbf{L}_k is the \mathbf{k}_{th} lighting pattern, $\mathbf{1}$ is an all-one vector and $S_1 = |\max(\mathbf{E})| + |\min(\mathbf{E})|$. Equation 7 describes how to shift and scale a basis function.

Then, the way to calculate the coefficients, c_k , to reconstruct the SRF becomes

$$c_k = \frac{S_1}{255} I_k(m, n) - \mathbf{e}_k^T \mathbf{m} - |\min(\mathbf{E})| \mathbf{F}^T \mathbf{1} \quad (8)$$

$\mathbf{F}^T \mathbf{1}$ in Equation 8 is $\frac{I_{gray}(m, n)}{128}$, where $I_{gray}(m, n)$ is a pixel value captured with the solid gray lighting pattern.

4. EXPERIMENT RESULTS

4.1. Performance of SRF Reconstruction

The proposed algorithm is compared with other relighting algorithms, which use an environment matte [3, 5, 4]. We apply a DCT-based approach and a PCA-based approach, and evaluate the performance. For test scenes to generate the error curves in Figure 5, ten different scenes are chosen as follows (Figure 6). Note that the training scenes used to create the PCA basis functions and test scenes are different except for the surface properties.

In Figure 7 (1), we generate the SRF reconstruction error curves using ten different diffused scenes by increasing the number of lighting patterns for our algorithm and method in [4, 5]. The error is computed in the mean-square sense. Figure 7 (2) compares the performance between our proposed methods and the methods in [4, 3] when ten different specular scenes are used as test scenes.

In Figure 7, the proposed methods outperform others [3, 5, 4]. From the result shown in Figure 7, a DCT-based approach fits better for Lambertian scenes. In signal processing literature [11], if a signal is an AR(1) process and the correlation parameter, ρ , of an AR(1) model is close to 1, the optimal basis functions for the signal approximate to

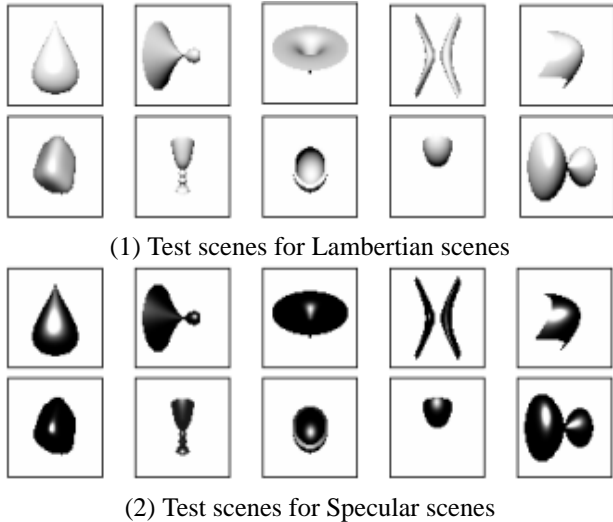


Figure 6: Test scenes

DCT basis functions. We can fit SRFs to an AR(1) and verify whether ρ is close to 1 or not by checking the significant level of the modified Li-McLeod portmanteau (LMP) statistic [13]. As a result, ρ estimated from Lambertian scenes is 0.9108 ± 0.1075 with 95% confidence intervals and ρ estimated from Specular scenes is 0.8321 ± 0.2425 with 95% confidence intervals. It shows that SRFs from Lambertian scenes fit better for an AR(1) process with ρ close to one and, therefore, a DCT-based approach fits better for Lambertian scenes.

4.2. Rendered images

Rendered images are presented in Figures 8 and 9. If the scene is Lambertian, our algorithm can provide very good quality of rendered images using only six basis images. For specular scenes, it is necessary to use more basis images corresponding to high order basis functions than Lambertian scenes. If the difference in Figures 8 and 9 is close to gray, the rendered image is close to the ground truth. Figure 8 shows that our method can generate better quality of rendered images than [4], even though we apply fewer patterns, six, than [4], 15 lighting patterns applied. In Figure 9, we choose 15 patterns for both algorithms and compare the quality of the rendered images. We compute the mean square error of the rendered image and show on the difference map. We can see that rendered images from a PCA-based algorithm are significantly closer to the ground truth than [4].

5. CONCLUSION

In this paper, we introduce a statistical approach to reconstructing SRFs. Our goal is to achieve efficiency as well as accuracy. The proposed technique obtains basis images by

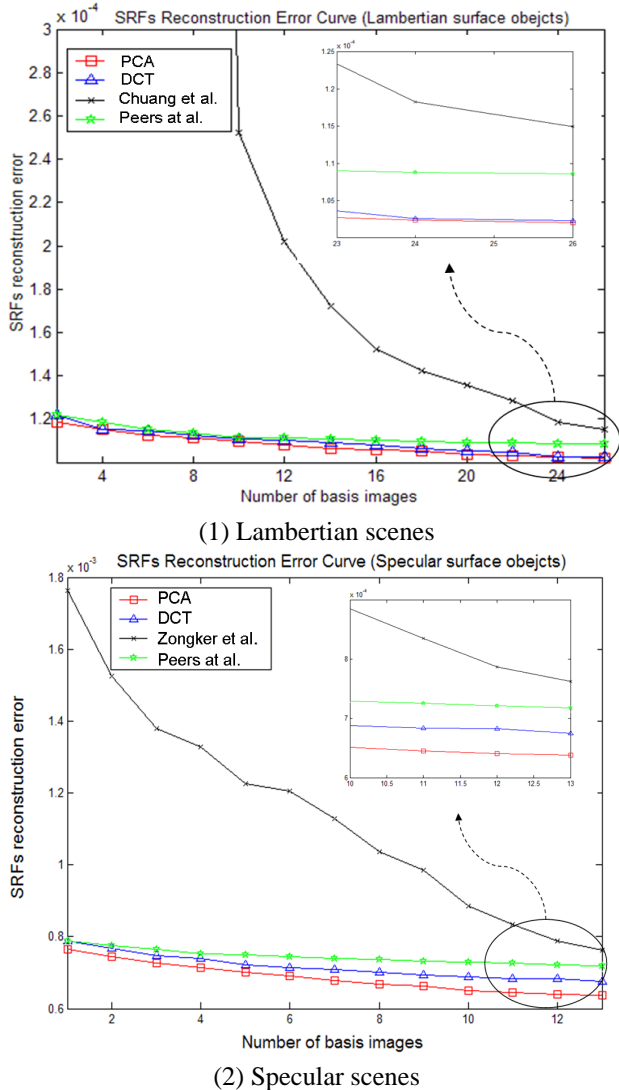


Figure 7: Comparison with other relighting algorithms

selecting the most effective lighting patterns. The property of selecting lighting patterns can be understood as a pre-compression algorithm for IBL. Since the proposed algorithm acquires the data set smartly, we do not have to store a large amount of data for IBL.

Reconstructed SRFs can be utilized in many other applications such as detecting the shadow or generating the normal map of a scene. This is very useful in object recognition and detection. Our future work will attempt to achieve both image-based relighting and multi-view rendering of the scene without prior knowledge of the geometry information, while using as few basis images as possible.

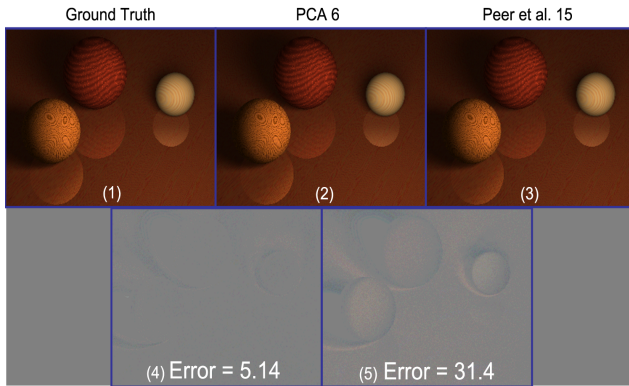


Figure 8: (1) Scene under true lighting(ground truth), (2) Rendered image by our proposed method using six images, (3) Rendered image by [6] using fifteen images, (4) Difference map between (1) and (2), (5) Difference map between (1) and (3)

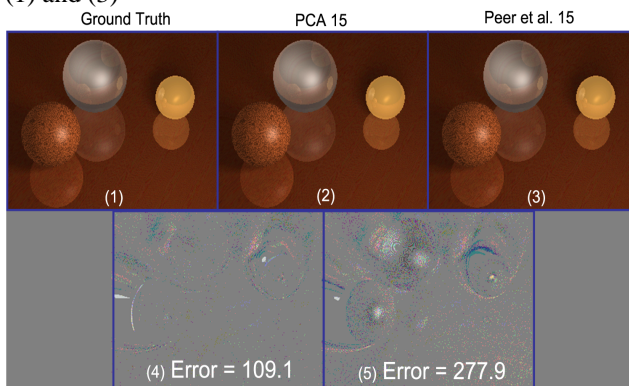


Figure 9: (1) Scene under true lighting(ground truth), (2) Rendered image by our proposed method using fifteen images, (3) Rendered image by [6] using fifteen images, (4) Difference map between (1) and (2), (5) Difference map between (1) and (3)

References

- [1] T. T. Wong, "Image-based relighting as the sampling and reconstruction of the plenoptic illumination function," *Proceedings of IEEE ICASSP*, pp. 764–767, 2003.
- [2] Z. Lin, T. T. Wong, and H. Y. Shum, "Relighting with the reflected irradiance field: Representation, sampling and reconstruction," *Proceedings of IEEE CVPR*, pp. 561–567, 2001.
- [3] D. E. Zongker, D. M. Werner, B. Curless, and D. H. Salesin, "Environment matting and compositing," *SIGGRAPH Conference Proceedings*, pp. 205–214, 1999.
- [4] P. Peers and P. Dutre, "Wavelet environment matting," *Eurographics Symposium on Rendering*, pp. 25–27, 2003.
- [5] Y. Y. Chuang, D. E. Zongker, J. Hindorff, B. Curless, D. H. Salesin, and R. Szeliski, "Environment matting extensions: Towards higher accuracy and real-time capture," *SIGGRAPH Conference Proceedings*, 2000.
- [6] P. Debevec, T. Hawkins, C. Tchou, H. P. Duiker, W. Sarokin, and M. Sagar, "Acquiring the reflectance field of a human face," *SIGGRAPH Conference Proceedings*, pp. 158–165, 2003.
- [7] J. Nimeroff, E. Simoncelli, and J. Dorsey, "Efficient re-rendering of naturally illuminated environments," *Fifth Eurographics Workshop on Rendering*, pp. 359–373, 1994.
- [8] P. M. Ho, T. T. Wong, K. H. Choy, and C. S. Leung, "PCA-based compression for image-based relighting," *Proceedings of IEEE ICME*, 2003.
- [9] V. Masselus, P. Peers, P. Dutre, and Y. Willems, "Smooth reconstruction and compact representation of reflectance functions for image-based relighting," *Eurographics Symposium on Rendering*, 2004.
- [10] O. D. Richard, E. H. Peter, and G. S. David, *Pattern Classification 2nd edition*, pp. 115–117.
- [11] A. K. Jain, *Fundamentals of Digital Image Processing*, pp. 152–154.
- [12] Copyright © 1994 ~ 2004 Hallam Oaks Pty. Ltd, "<http://www.povray.org/>," .
- [13] Copyright ©2001 Association for Computing Machinery, "<http://www.gps.caltech.edu/~tapio/arfit/>," .